Table of Contents

Abbreviations

2,3-DHBA 2,3-dihydroxybutyric acid
2M3HBA 2-methyl-3-hydroxybutyric acid
2M3HPA 2-methyl-3-hydroxypentanoic acid
3,4-DHBA 3,4-dihydroxybutyric acid
3-HBA 3-hydroxybutyrate
3-HBA-CoA 3-hydroxybutyryl-CoA
3-HPA 3-hydroxypentanoic acid
ΔNPduP N-terminal truncated version of CoA-acylating aldehyde dehydrogenase from *Salmonella enterica*
β-BOX Reverse β-oxidation pathway
ADH Alcohol dehydrogenase
AG Crosslinked agarose microbeads
AG-Co^{2+} Agarose functionalized with Cobalt chelates groups
AG-Co^{2+}/G/A Agarose functionalized with Cobalt chelates, aldehydes, and amine groups
AG-G Agarose functionalized with glyoxyl groups
AG-PAH Agarose functionalized with polyallylamine
AG-PEI Agarose functionalized with polyethyleneimine
Alexa Alexa Fluor 647 NHS ester
AsAcat5 Thiolase 5 from *Ascaris suum*
ATP Adenosine 5'-triphosphate
Atto Atto 390 NHS ester
BMC Bacterial microcomparment
BsADH Alcohol dehydrogenase from *Bacillus stearothermophilus*
BsGDH Thermal stable variant of glucose dehydrogenase from *Bacillus subtilis*
CLSM confocal laser scanning microscopy
CoA Coenzyme A
DTNB (Ellman's Reagent) (5,5-dithio-bis-(2-nitrobenzoic acid)
DTT Dithiothreitol
EAA Ethyl acetoacetate
EcTesB Thioesterase B from *Escherichia coli*
Ee Enantiomeric excess
FAD^+ Flavin adenine dinucleotide
FITC Fluorescein isothiocyanate
GaNOX NADH oxidase from *Granulicatella adiacens*
GC/MS Gas chromatography coupled to mass spectroscopy
HB Heterogeneous biocatalyst
HPLC: High-performance liquid chromatography
IPTG Isopropyl β-D-thiogalactoside
LB Luria broth
LpNOX NADH oxidase from *Lactobacillus pentosus*
$NaBH_4$ Sodium borohydride
HisTag Histidine tag
NADH Nicotinamide adenine dinucleotide (reduced form)
NAD^+ Nicotinamide adenine dinucleotide (oxidized form)
NADPH Nicotinamide adenine dinucleotide phosphate (reduced form)
$NADP^+$ Nicotinamide adenine dinucleotide phosphate (oxidized form)
NOX NADH oxidase
PAH Poly(allylamine)
PBR Packed-bed reactor
PduP CoA-acylating aldehyde dehydrogenase
PEI Poly(ethyleneimine)
ReTHL Thiolase from *Ralstonia eutropha*
RhB Rhodamine B isothiocyanate
SePduP CoA-acylating aldehyde dehydrogenase from *Salmonella enterica*
ScADH Alcohol dehydrogenase from *Saccharomyces cerevisiae*
STY Space time yield
TB Terrific Broth
TCEP Tris(2-carboxyethyl)phosphine
THBA 2,3,4-trihydroxybutyric acid
TtHBDH 3-hydroxybutyryl-CoA dehydrogenase from *Thermus thermophilus*
TTN Turnover number

UPLC/MS Ultra high-performance liquid chromatography coupled to mass spectroscopy
WT Wild type

Supplementary Tables

Table S1. Primers to truncate pdu gene

Primer name	Primer sequence (5'-3')
ΔNPduP_fw	AACATATGGGCAAGGGCATTTTCCAGAGCGTG
ΔNPduP_rv	CAGGATCCTTAACGGATGCTAAAACCGTTGGTC

Table S2. Protein sequences of enzymes used in this work

Protein name	Protein sequence
BsADH	MGSSHHHHHHSSGLVPRGSHMEFKRSMKAAVVEQFKEPLKIKEVEKPTISYGEVLVR IKACGVCHTDLHAAHGDWPVKPKLPLIPGHEGVGIVEEVGPGVTHLKVGDRVGIPWL YSACGHCDYCLSGQETLCEHQKNAGYSVDGGYAEYCRAAADYVVKIPDNLSFEEAA PIFCAGVTTYKALKVTGAKPGEWVAIYGIGGLGHVAVQYAKAMGLNVVAVDIGDEKLE LAKELGADLVVNPLKEDAAKFMKEKVGGVHAAVVTAVSKPAFQSAYNSIRRGGACVL VGLPPEEMPIPIFDTVLNGIKIIGSIVGTRKDLQEALQFAAEGKVKTIIEVQPLEKINEVF DRMLKGQINGRVVLTLEDK
SePduP	MGSSHHHHHHSSGENLYFQGHMKKLKRSNTSELETLIRTILSEQLTTPAQTPVQPQG KGIFQSVSEAIDAAHQAFLRYQQCPLKTRSAIISAMRQELTPLLAPLAEESANETGMG NKEDKFLKNKAALDNTPGVEDLTTTALTGDGGMVLFEYSPFGVIGSVAPSTNPTETIIN NSISMLAAGNSIYFSPHPGAKKVSLKLISLIEEIAFRCCGIRNLVVTVAEPTFEATQQMM AHPRIAVLAITGGPGIVAMGMKSGKKVIGAGAGNPPCIVDETADLVKAAEDIINGASFD YNLPCIAEKSLIVVESVAERLVQQMQTFGALLLSPADTDKLRAVCLPEGQANKKLVGK SPSAMLEAAGIAVPAKAPRLLIALVNADDPWVTSEQLMPMLPVVKVSDFDSALALALK VEEGLHHTAIMHSQNVSRLNLAARTLQTSIFVKNGPSYAGIGVGGEGFTTFTIATPTG EGTTSARTFARSRRCVLTNGFSIR
ΔNPduP	MGSSHHHHHHSSGLVPRGSHMGKGIFQSVSEAIDAAHQAFLRYQQCPLKTRSAIISA MRQELTPLLAPLAEESANETGMGNKEDKFLKNKAALDNTPGVEDLTTTALTGDGGM VLFEYSPFGVIGSVAPSTNPTETIINNSISMLAAGNSIYFSPHPGAKKVSLKLISLIEEIAF RCCGIRNLVVTVAEPTFEATQQMMAHPRIAVLAITGGPGIVAMGMKSGKKVIGAGAG NPPCIVDETADLVKAAEDIINGASFDYNLPCIAEKSLIVVESVAERLVQQMQTFGALLLS PADTDKLRAVCLPEGQANKKLVGKSPSAMLEAAGIAVPAKAPRLLIALVNADDPWVTS EQLMPMLPVVKVSDFDSALALALKVEEGLHHTAIMHSQNVSRLNLAARTLQTSIFVKN GPSYAGIGVGGEGFTTFTIATPTGEGTTSARTFARSRRCVLTNGFSIR
AsTHL5	MGSSHHHHHHSSGENLYFQGHMKKLKRSGTGMDAGKKDVYILSAVRTPIASFRSTL TSLSAVDLGIVVTKEAIKRSLLPSSAIEETIVGNVLSAGLGQNIARQISIASEIPKSSQCV TINKVCSSSMKAIIMGAQAIQVGYRRIVVALGSESMSNAPFYVPRGEIPFGGVQLVDA LQRDGLMDSIEYQPMGLCAEKTVKDYAFTREQLDAYAIESYRKAEHAWKEGAFNKEV VPVSVPQKRGSKVVLTEDEEYKRLIPEKVPALHPAFLKDGSGTITAANASTINDGAAA CVLASGEVVQEGRLKPIAKVLSYAEAGVEPIDFTVAPALAVKQLLSQSGLDEESIALWE INEAFSVTGLAFIKELRLDPKRVNVRGGAVALGHPLGASGARIVVTLVHALKSDELGVA AICNGGGEASAILIKKLGS
ReTHL	MGSSHHHHHHSSGLVPRGSHMEFKRSMTREVVVVSGVRTAIGTFGGSLKDVAPAEL GALVVREALARAQVSGDDVGHVVFGNVIQTEPRDMYLGRVAAVNGGVTINAPALTVN RLCGSGLQAIVSAAQTILLGDTDVAIGGGAESMSRAPYLAPAARWGARMGDAGLVD MMLGALHDPFHRIHMGVTAENVAKEYDISRAQQDEAALESHRRASAAIKAGYFKDQI VPVVSKGRKGDVTFDTDEHVRHDATIDDMTKLRPVFVKENGTVTAGNASGLNDAAA AVVMMERAEAERRGLKPLARLVSYGHAGVDPKAMGIGPVPATKIALERAGLQVSDLD VIEANEAFAAQACAVTKALGLDPAKVNPNGSGISLGHPIGATGALITVKALHELNRVQG RYALVTMCIGGGQGIAAIFERI
TtHBDH	MEVKRIGVVGAGQMGSGIAQVAASAGYEVVLVDVAESFLERGLAAIRRSLGKFLEKG KITQEAHDEALGRIRTSLSLEDLKDADLIVEAIVEDEGEKRRLFERLGALAKPEAILASN TSSIPITALARYSGRPERFIGMHFFNPVPLMQLVEVIRGELTSEATRDVVVEVARRMG KTPLEVQDYPGFISNRLLMPMINEAIEALREGVATKEAIDGIMRLGMNHPMGPLELAD FIGLDTCLAIMEVLHRGFGDDKYRPSPLLRRMVQAGLLGRKAGRGFYTYDEKGNKV G
EcTesB	MGSSHHHHHHSSGENLYFQGHMKKLKRSSQALKNLLTLLNLEKIEEGLFRGQSEDL GLRQVFGGQVVGQALYAAKETVPEERLVHSFHSYFLRPGDSKKPIIYDVETLRDGNS FSARRVAAIQNGKPIFYMTASFQAPEAGFEHQKTMPSAPAPDGLPSETQIAQSLAHLL PPVLKDKFICDRPLEVRPVEFHNPLKGHVAEPHRQVWIRANGSVPDDLRVHQYLLGY ASDLNFLPVALQPHGIGFLEPGIQIATIDHSMWFHRPFNLNEWLLYSVESTSASSARG FVRGEFYTQDGVLVASTVQEGVMRNHN
LpNOX	MGSSHHHHHHSSGLVPRGSHMKVIVIGCTHAGTAAVNQILASNPETDVTIYERNDNV SFLSCGIALYLGGEVADPQGLFYSSPEQLAKLGANVHMQHDVTDVDTENHEITVTDL KTGESKKDYYDKLVVTTGSWPVIPPIDGIDSPNVYLCKNWTHAQSLWEAAKPAKRVIV IGGGYIGTELVEAYQKQGKEVTLIDGLPRILNKYLDKGFTDRVEKDFVDHGIKMALNQ MVKGFSDDGKEVTVKTDKGSYTADMAILCVGFRPNTSLLKGKVDMNPNGSIKTNDY MQTSDPDIYGAGDSVAVHYNPTKKDAYIPLATNAVRQGTLVGLNIFKPTRKYMGTQST SGLMLFGKTIVSSGMTLEHAQAEKVPAEAVTFEDNYRPEFMPTTKPVLMQLVYNPET REILGAQFMSEHDVSQSANVISVMIQNHNTIDDLGFVDMFFQPIYDRPFNYLNLLGQA AIAHAAEKVTE
GaNOX	MGSSHHHHHHSSGLVPRGSHMKVVVVGCTHAGTAAVKTILNDNPGTEVVVYERND NVSFLSCGIALYVGGVVKDPQGLFYSSPEELASLGATVRMEHDVTSIDTVGKTLTVKD LKTGEEKTDSFDKLVLTTGSWPILPPIPGRELENVQLCKNYNQAKEIFAKKTDKKKVV

	VVGGGYIGIELVEAFALEGKEVTLVDGLDRILNKYLDPEFTDILEEDLRARGVQVRLNE MVKSFEGENGVVNKVVTSGGEYEADMVILCVGFRPNNDLVKDQLETMPNGAIIVND YMETSVKDVYAAGDSCAVNYNPNGGHAYIPLATNAVRMGSLVGKNINGHKVKYRGT QSTSGLHLFGWNIGSTGVNVGSAPHFGLDVRSVYVVDNHRPEFMPTYEKIYMKLVY EVGTNRIVGGQVMSKYDCTASANTLSLAIQNKMTIEDLAYVDFFFQPVFDRPWNYLNI LGQAAVEQERVLAEGK
BsGDH	MGSSHHHHHHSSGLVPRGSHMYPDLKGKVVAITGAASGLGKAMAIRFGKEQAKVVI NYYSNKQDPNEVKEEVIKAGGEAVVVQGDVTKEEDVKNIVQTAIKEFGTLDIMINNAG LENPVPSHEMPLKDWDKVIGTNLTGAFLGSREAIKYFVENDIKGNVINMSSVHEVIPW PLFVHYAASKGGIKLMTKTLALEYAPKGIRVNNIGPGAINTPINAEKFADPKQKADVES MIPMGYIGEPEEIAAVAAWLASKEASYVTGITLFADGGMTLYPSFQAGRG

Table S3. Chemical structure of aldehydes and alcohols tested in this work.

Alcohols	Aldehydes	
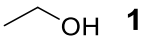 **1a**	 **2a**	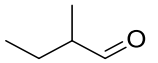 **2j**
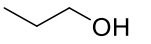 **1b**	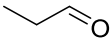 **2b**	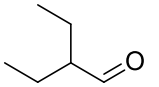 **2k**
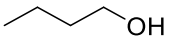 **1c**	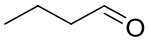 **2c**	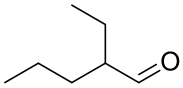 **2l**
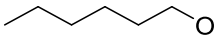 **1d**	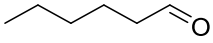 **2d**	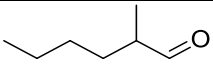 **2m**
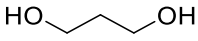 **1n**	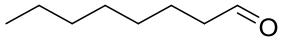 **2e**	
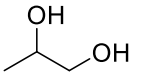 **1o**	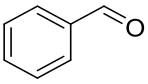 **2f**	
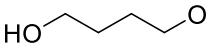 **1p**	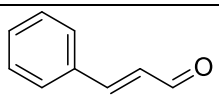 **2g**	
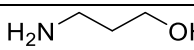 **1q**	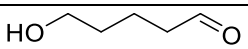 **2h**	
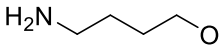 **1r**	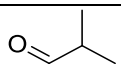 **2i**	

Table S4. Immobilization parameters for all individually immobilized enzymes described in this work.

Enzyme	Carrier	Immobilization Yield[a] (%)	Expressed Activity[b] (%)	Immobilization Efficiency[c] (%)
ΔNPduP	AG-G	99	21.5	18.0
	Co^{2+}-Agarose	100	8.6	8.6
	PAH-A	67	47.9	45.9
	AG-Co^{2+}/G/A	98	8.3	8.5
BsADH	Glyoxyl-Agarose	100	36.6	36.6
	Co^{2+}-Agarose[d]	100	19	19
	PEI-A	100	99.2	99.2
	AG-Co^{2+}/G/A[d]	100	30	30
GaNOX	Glyoxyl-Agarose	97	2.9	2.8
	Co^{2+}-Agarose	95	53.3	51.0
	PEI-A	82	60.8	49.9
	AG-Co^{2+}/G/A	100	5.3	5.3

[a] Immobilization yield (%) = 100 × (1 − (volumetric activity in the supernatant upon the immobilization/volumetric offered activity)). [b] Expressed activity (%) = (measured activity upon the immobilization per gram of carrier) / (offered activity per mass of carrier × (immobilization yield/100)) × 100. [c] Immobilization efficiency (%) = 100 x measured activity per mass of carrier upon the immobilization/offered activity per mass of carrier.[d] Results obtained from Santiago-Arcos et al. 2023.[1]

Table S5. Immobilization parameters for all multi-functional heterogeneous biocatalysts described in this work.

Name	Enzyme	Chemistry	Yield[a] (%)	Apparent immobilization efficiency[b] (%)	Offered activity (U g^{-1})	Apparent recovered activity (U g^{-1})
HB-1	BsADH	Glyoxyl	99.3	4.8	16	0.77
	ΔNPduP		92.9	1.3	9.16	0.12
	GaNOX	PEI	90	105.3	19	20
HB-2.1	BsADH	Glyoxyl	100	0.7	130	0.88
	ΔNPduP		99.7	0.5	23	0.12
HB-2.2	BsADH	Glyoxyl	100	2.5	26	0.66
	ΔNPduP		99.7	1.0	23	0.22
HB-2.3	BsADH	Glyoxyl	100	5.2	5.2-100	0.27
	ΔNPduP		99.7	2.8	23-500	0.65
HB-3	AsTHL5	Cobalt chelates	-	-	-	0.5
HB-4	TtHBDH	Glyoxyl	100	11	7.53	0.828
	EcTesB		100	9.4	4.52	0.43
	BsGDH		100	37	28.4	10.5
HB-5	AsTHL5	Cobalt chelates	-	-	-	0.25-0.5
	TtHBDH		-	-	-	0.9-1.1
	EcTesB		-	-	-	0.3-0.5
HB-6	BsADH	Cobalt chelates	-	-	-	0.69
	ΔNPduP		-	-	-	0.1
	AsTHL5		-	-	-	0.72
	TtHBDH		-	-	-	1.3
	EcTesB		-	-	-	1.1
HB-7	ReTHL	Glyoxyl		9.9	6.48	0.644
	TtHBDH			3.25	36	1.17
	EcTesB			8.4	12.1	1.02
HB-8.1	BsADH	Glyoxyl		0.63	235	1.48
	ΔNPduP			0.021	540	0.115
	ReTHL			7.4	6.48	0.481
	TtHBDH			4	36	1.43
	EcTesB			11.7	12.1	1.42
HB-8.2	BsADH	Glyoxyl		0.85	142	1.2
	ΔNPduP			0.037	800	0.298
	ReTHL			1.8	5.6	0.1
	TtHBDH			1.6	43	0.674
	EcTesB			19	1.05	0.2

[a] Immobilization yield (%) = 100 × (1 − (amount of protein in the supernatant upon the immobilization/offered amount of protein)). [b] Apparent immobilization efficiency (%) = 100 x measured activity upon the immobilization/offered activity

Table S6. Kinetic Parameters of soluble enzymes

Enzyme	Reaction	K_{eq} (ΔG^m / kJ mol^{-1})[a]	K_m (mM)
BsADH	Acetone + NADH = IPA + NAD	2 (-1.7)	Acetone – 5.88
			NADH – 0.0768
			IPA – 46.1
			NAD^+ – 0.08
	Ethanol + NAD = AcCHO + NADH	0.0015 (16.1)	Ethanol – 1.49
			NAD^+ – 0.08
			AcCHO – 0.034
			NADH – 0.0768
ΔNPduP	AcCHO + NAD + CoA = AcCoA + NADH	23000 (-7.7)	AcCHO – 2.943
			CoA – 0.0477
			NAD^+ – 0.466
			AcCoA – 0.3421
			NADH – 0.1
AsTHL5	2 AcCoA = AcAcCoA + CoA	0.00025 (26.3)	AcCoA – 0.33
			AcAcCoA – 0.02
			CoA – 0.0085
ReTHL	2 AcCoA = AcAcCoA + CoA		AcCoA – 0.0258
			AcAcCoA – 0.158
			CoA – 0.1
TtHBDH	AcAcCoA + NADH = 3HBCoA + NAD	40 (-9.3)	AcAcCoA – 0.1
			NADH – 0.0334
			3HBCoA – 0.015
			NAD^+ – 0.186
EcTesB	3HBCoA -> 3-HBA + CoA	3900000 (-54.7)	3HBCoA – 0.33
	AcCoA -> Ac + CoA	1800000 (-52.7)	AcCoA – 0.2

[a]Values calculated using eQuilibrator at pH 8, pMg 2, and ionic strength of 0.2 M. For COPASI model construction, water (H_2O) was omitted to simplify the models. Abbreviations: IPA-Isopropanol; AcCHO-Acetaldehyde; AcCoA: Acetyl-CoA; AcAcCoA-Acetoacetyl-CoA; 3HBCoA-3-hydroxybutyryl-CoA; Ac-Acetate.

Table S7. Kinetic functions for COPASI modelling

General reaction formula	Kinetic function	Enzymes to which the function applies
A + B = P + Q	$V = \frac{\frac{V_{max} \times \left(A\ x\ B - \frac{P\ x\ Q}{K_{eq}}\right)}{K_A\ x\ K_B}}{\left(1 + \frac{A}{K_A}\right)\ x\ \left(1 + \frac{B}{K_B}\right) + \left(1 + \frac{P}{K_P}\right)\ x\ \left(1 + \frac{Q}{K_Q}\right) - 1}$	BsADH (Ethanol and Acetone), TtHBDH,
A + B + C = P + Q	$V = \frac{\frac{V_{max} \times \left(A\ x\ B\ x\ C - \frac{P\ x\ Q}{K_{eq}}\right)}{K_A\ x\ K_B\ x\ K_C}}{\left(1 + \frac{A}{K_A}\right)\ x\ \left(1 + \frac{B}{K_B}\right)\ x\ \left(1 + \frac{C}{K_C}\right) + \left(1 + \frac{P}{K_P}\right)\ x\ \left(1 + \frac{Q}{K_Q}\right) - 1}$	ΔNPduP
A -> B + C	$V = \frac{V_{max}\ x\ A}{K_A + A}$	EcTesB (3-HB-CoA and Acetyl-CoA)
A = B + C	$V = \frac{\frac{V_{max} \times \left(A - \frac{P\ x\ Q}{K_{eq}}\right)}{K_A}}{\left(1 + \frac{A}{K_A}\right) + \left(1 + \frac{P}{K_P}\right)\ x\ \left(1 + \frac{Q}{K_Q}\right) - 1}$	ReTHL

Table S8. COPASI modelling

Model version	Enzyme	Loading (U mL^{-1})	Reaction conditions	Predicted 3-HBA (mM)	Predicted acetate (mM)
Model 1.0	BsADH	1 (**1a**)	200 mM ethanol, 300 mM acetone, 1 mM NAD^+, 1 mM CoA	3.4	88
		0.7 (acetone)			
	ΔNPduP	1			
	ReTHL	1			
	TtHBDH	1			
	EcTesB	1 (**5a**)			
		0.15 (**3a**)			
Model 1.1	BsADH	2.5 (**1a**)	200 mM ethanol, 300 mM acetone, 1 mM NAD^+, 1 mM CoA	44	17.4
		1.75 (acetone)			
	ΔNPduP	10			
	ReTHL	0.25			
	TtHBDH	2.5			
	EcTesB	0.1 (**5a**)			
		0.015 (**3a**)			
Model 1.2	BsADH	1 (**1a**)	200 mM ethanol, 300 mM acetone, 1 mM NAD^+, 1 mM CoA	58	16.7
		0.7 (acetone)			
	ΔNPduP	40			
	ReTHL	0.1			
	TtHBDH	1			
	EcTesB	0.1 (**5a**)			
		0.015 (**3a**)			

Supplementary Figures

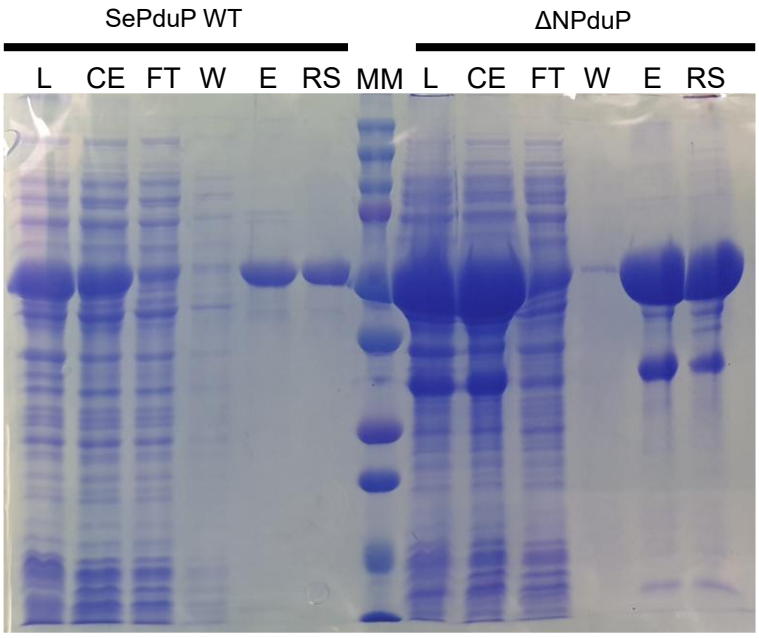

Figure S1. SDS-PAGE of SePduP WT and ΔNPduP purification. Abbreviations: MM (Molecular weight markers, BioRad Precision Plus Protein All Blue Standard). L (lysate), CE (soluble crude extract), FT (flow-through of the purification), W (washing buffer after flow-through), E (eluted protein), and RS (washed resin after purification).

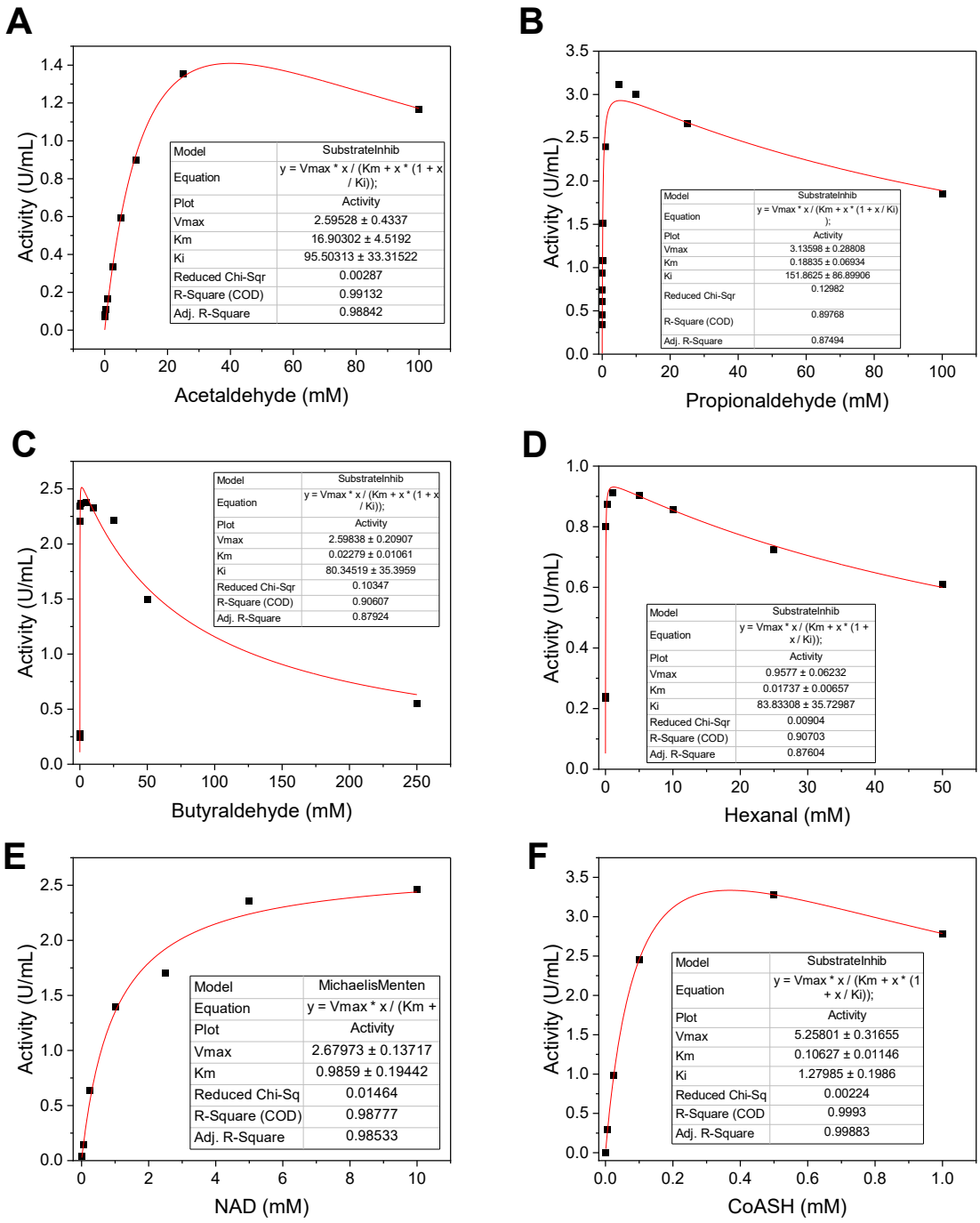

Figure S2. Michaelis-Menten curves of ΔNPduP for different substrates or cofactors. Oxidative steady-state kinetics were calculated towards A) Acetaldehyde (0-100 mM), B) Propionaldehyde (0-100 mM), C) Butyraldehyde (0-250 mM), D) Hexanal (0-50 mM), E) NAD^+ (0-10 mM), and CoA (0-1 mM). The activities for each substrate concentration were done in triplicate, resulting in a mean value for each substrate concentration. All mean activities were plotted and adjusted to a substrate inhibition model (except NAD^+), which was fitted to a Michaelis-Menten model) using Origin Pro 2020 software.

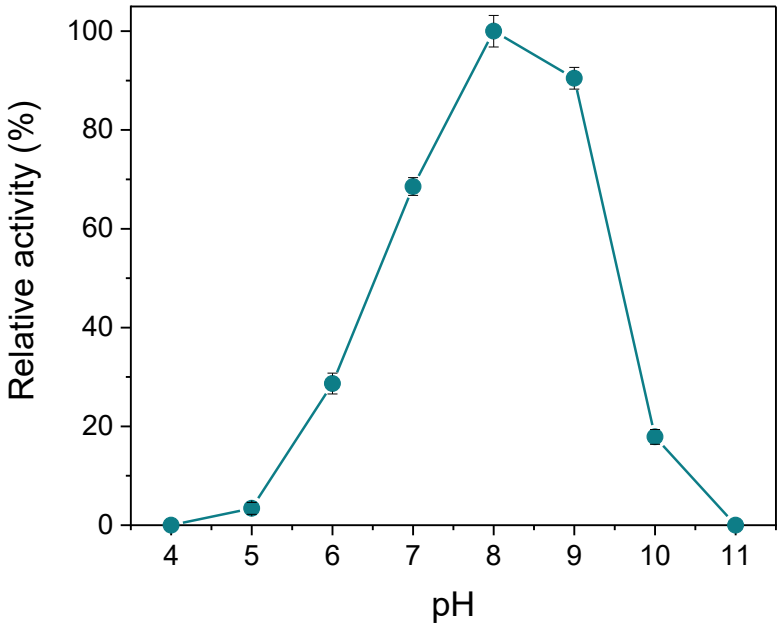

Figure S3. ΔNPduP activity vs pH. Activity assays were performed as described in the Methods section. 0.1 M acetate buffer was used for pH 4 and 5; 0.1 M phosphate buffer was used for pH 6 to 8, and 0.1 M bicarbonate buffer was used for pH 9 to 11.

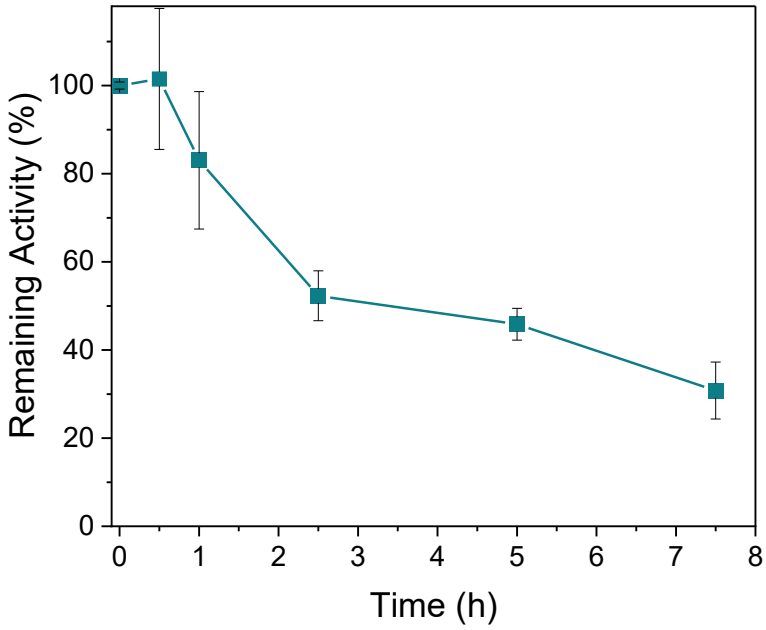

Figure S4. Thermal inactivation assay of ΔNPduP at 65 ºC in 0.1 M phosphate buffer pH 7.

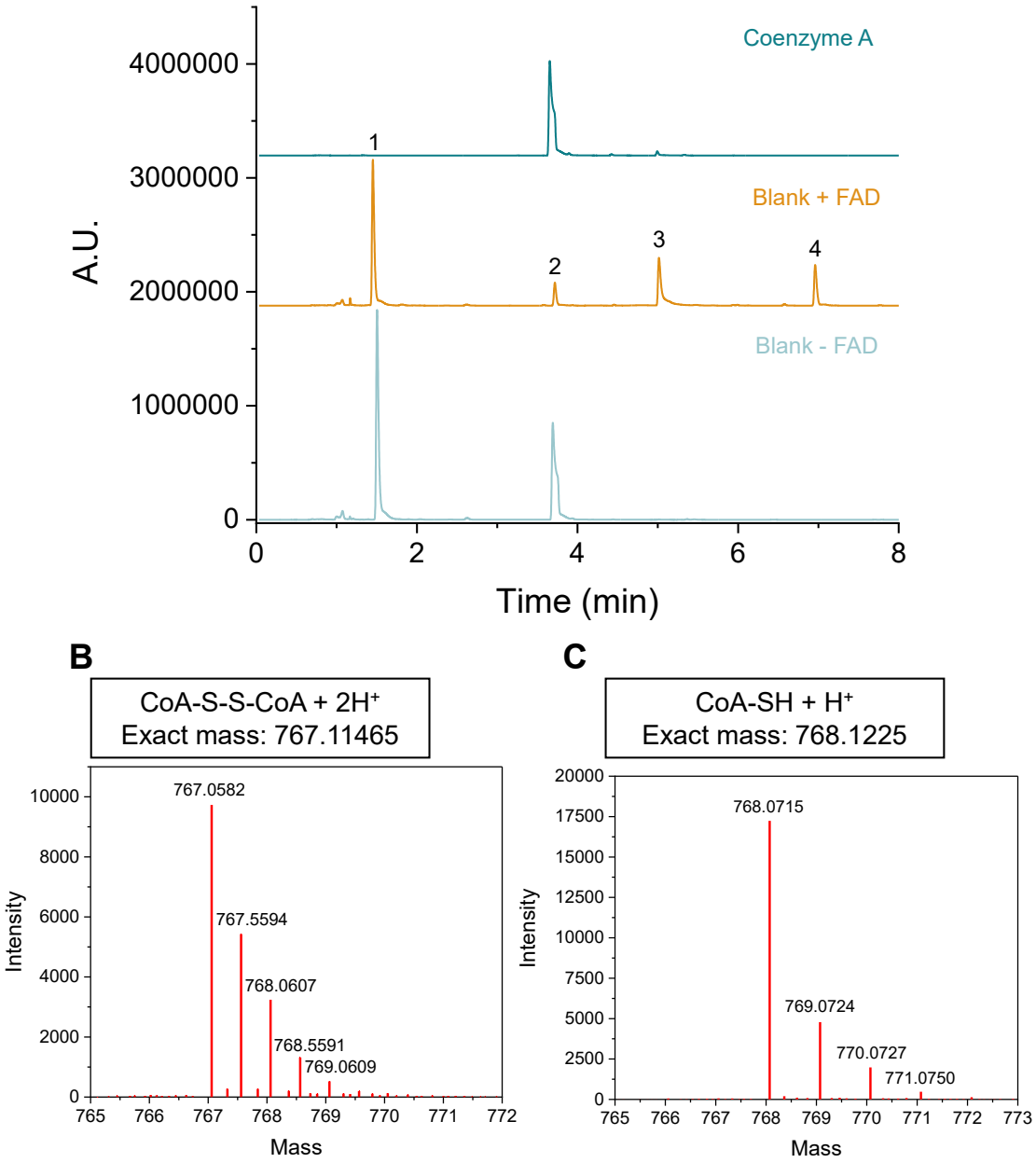

Figure S5. UPLC-MS chromatograms and MS spectra. A) UV chromatograms (254 nm) of 1 mM of Coenzyme A (upper chromatogram); blank with 1 mM CoA, 1 mM NAD^+, 1 mM DTT and 0.15 mM FAD^+ (middle chromatogram); blank with 1 mM CoA and 1 mM NAD^+ and 1 mM DTT (lower chromatogram). Peak 1 – NAD^+; Peak 2 – Coenzyme A; Peak 3 – Coenzyme A dimer; Peak 4 – FAD^+. B) Mass spectra of Peak 3 in blank with FAD. C) Mass spectra of Peak 2 in blank with FAD^+.

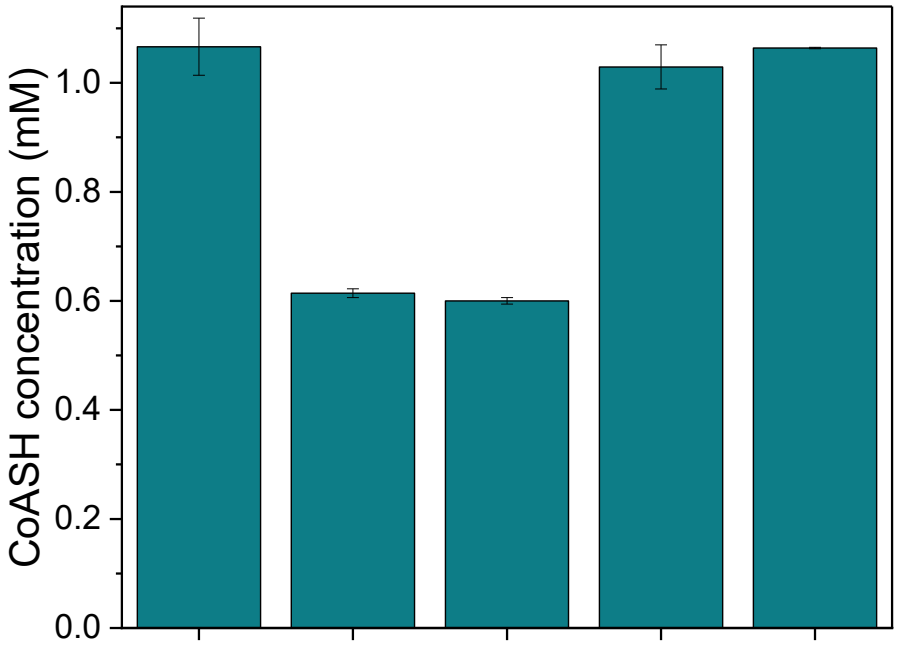

Entry	1	2	3	4	5
NAD^+ (mM)	2.5	0.1	0.1	0.1	2.5
DTT	+	+	+	+	
TCEP					+
NOX			Lp	Lp	
FAD		+	+		

Figure S6. Controls without ΔNPduP of the synthesis of propionyl-CoA from propionaldehyde in presence of excess of NAD^+ or NOX enzymes. The reactions were performed as described in Methods section. Lp indicates the presence of *Lactobacillus pentosus* NADH oxidase.

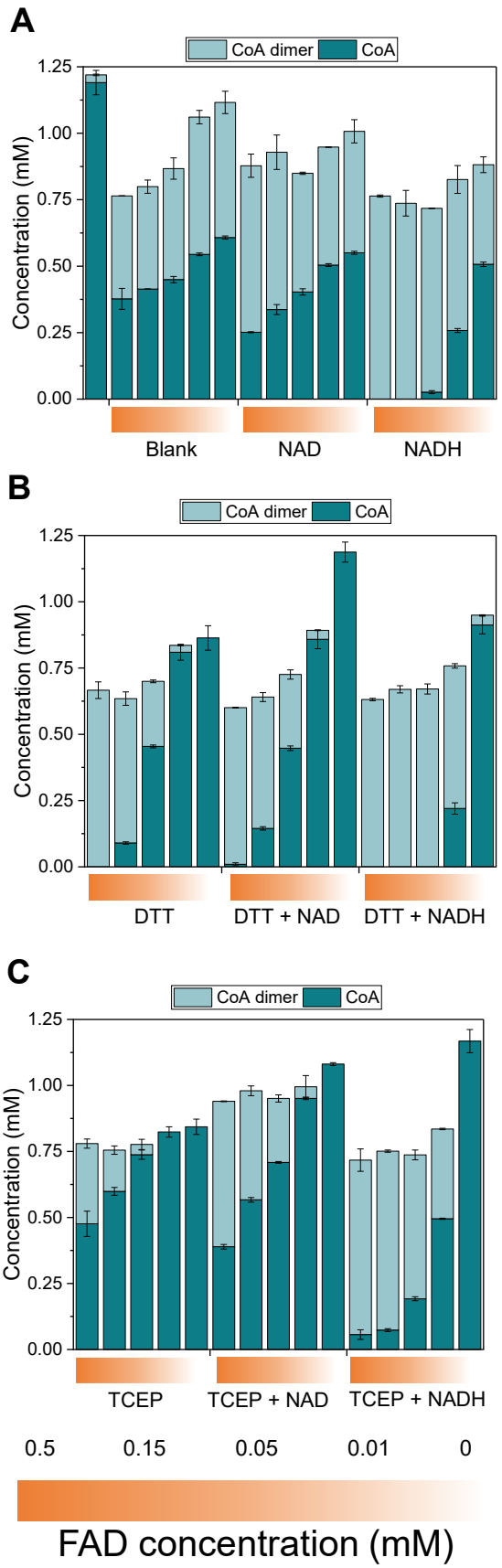

Figure S7. Incubation of Coenzyme A with different concentrations FAD^+ in the presence of different of either DTT, TCEP, NAD or NADH. A) Incubations in absence of either TCEP or DTT. B) Incubations in presence of 1 mM DTT. C) Incubations in presence of 1 mM TCEP. The incubations were done and analyzed as described in the Methods section.

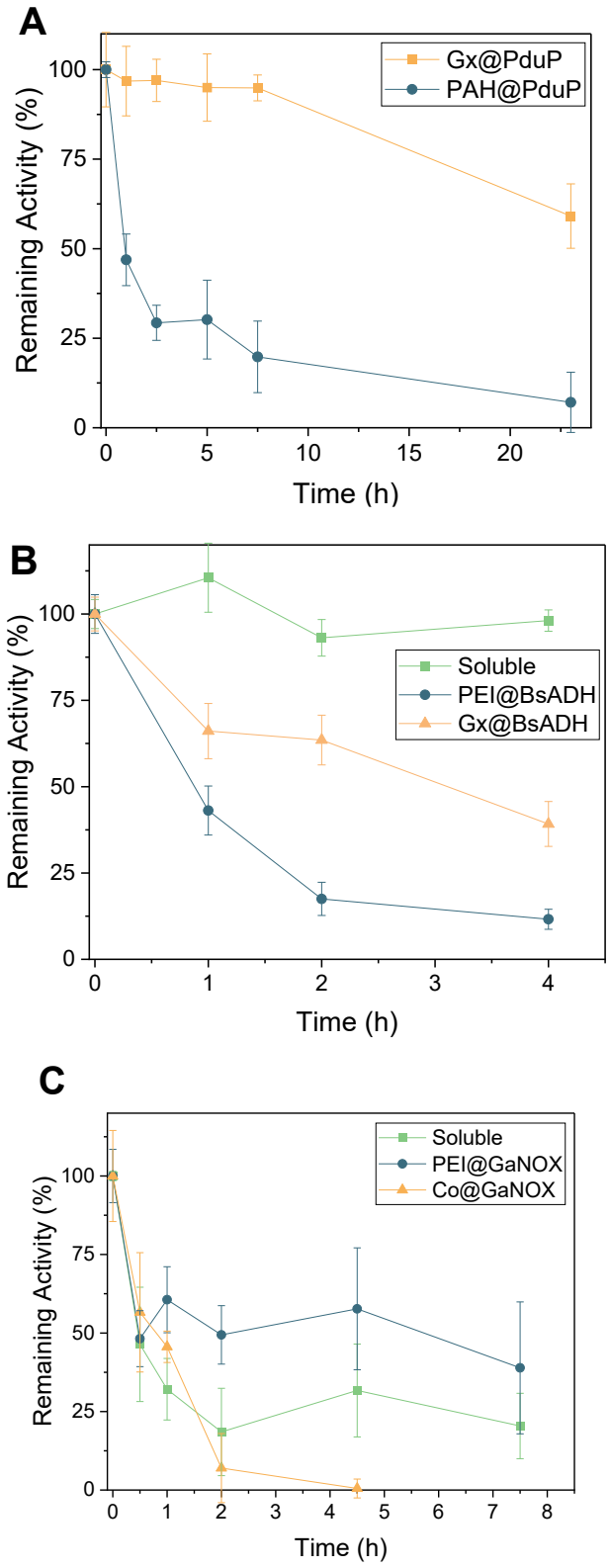

Figure S8. Thermal inactivation assay of A) ΔNPduP biocatalysts at 65 ºC in 0.1 M phosphate buffer pH 8, B) BsADH biocatalyst at 65 ºC in 0.1 M phosphate buffer pH 8 and C) GaNOX biocatalysts at 40 ºC in 0.1 M phosphate buffer pH 8.

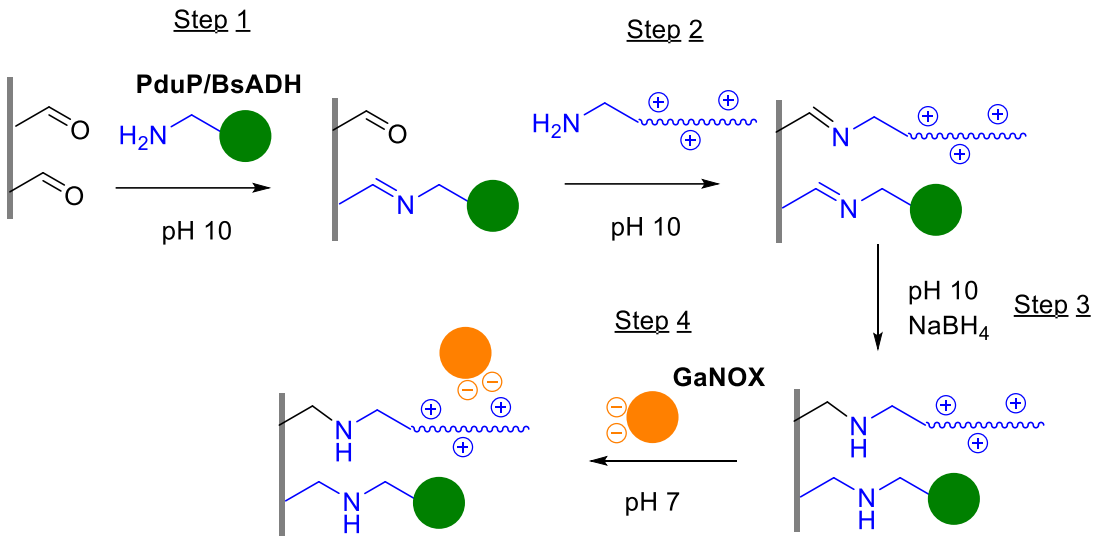

Figure S9. Schematic representation of the preparation of Heterogeneous Biocatalyst 1 (HB-1).

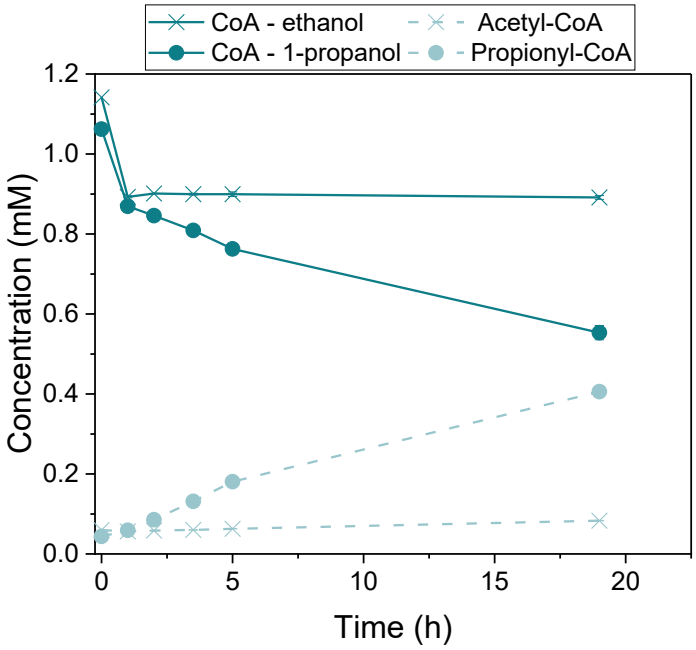

Figure S10. Time-course of the oxidative thioesterification of ethanol (crosses) and 1-propanol (circles) catalyzed in presence of 10 μM NAD^+ by HB-1 at pH 8, 30 ºC and 800 rpm. Reactions were done as indicated in the Methods section.

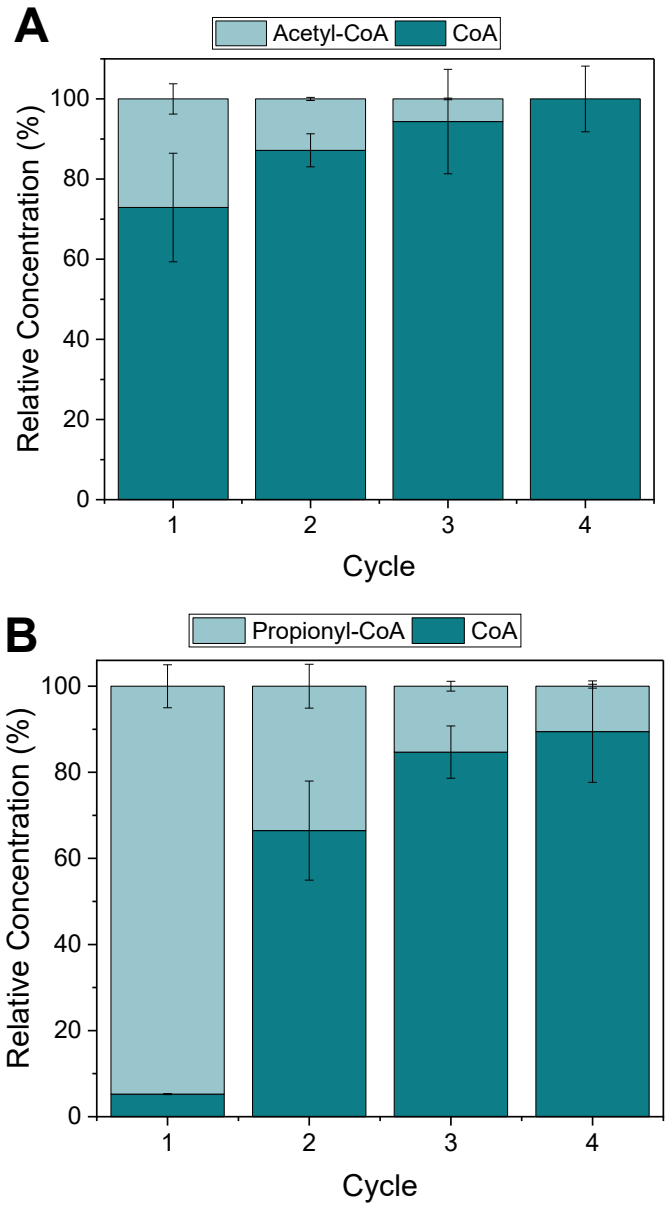

Figure S11. Consecutive oxidative thioesterification of 10 mM of A) ethanol or B) 1-propanol catalyzed in presence of 0.1 mM NAD^+ by HB-1 at pH 8, 30 ºC and 800 rpm for 5 hours per cycle. Reactions were done as indicated in the Methods section.

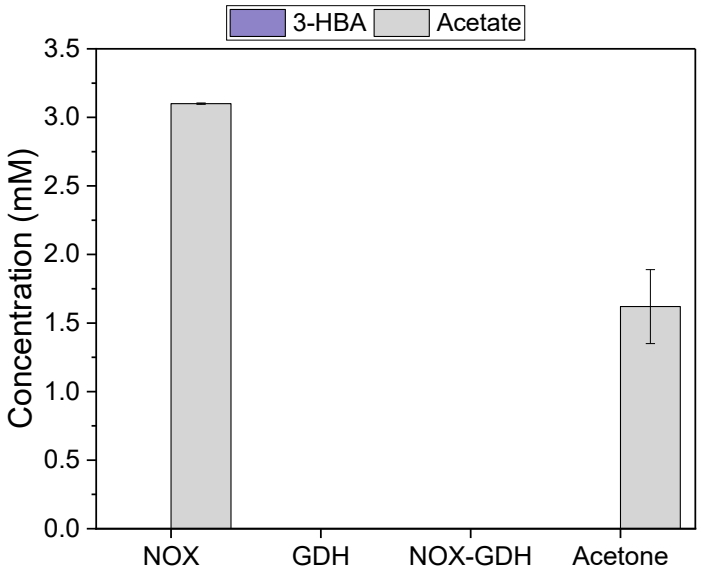

Figure S12. Comparison of different NAD(H) regeneration system towards the biosynthesis of 3-HBA from ethanol in homogeneous media. The reactions were performed as described in Methods section. Reactions containing BsGDH also contain 100 mM glucose in the reaction media.

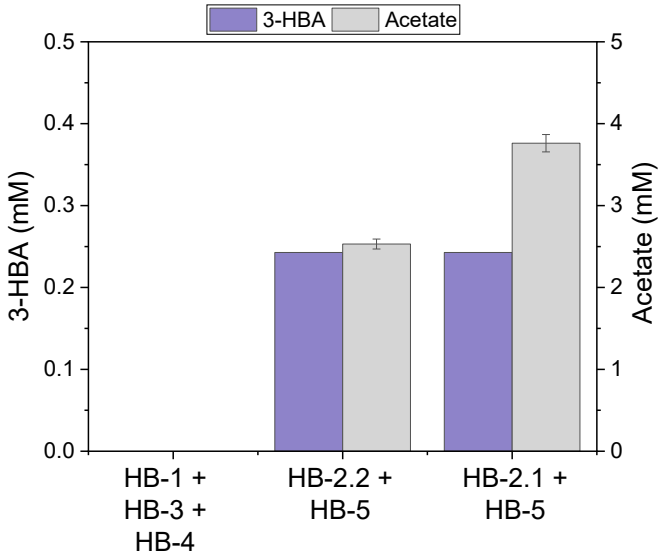

Figure S13. Comparison of different spatial organizations of the enzymatic pathways that transform ethanol into 3-HBA. 15 mg HB-1, 30 mg of HB-4 and 25 mg of HB-5 for the reaction on the left side of the graph; 25 mg of HB-2.2 or HB-2.3 and HB-3 were added to their corresponding reaction. Reactions were triggered by resuspending the HBs into the reaction media to a final ratio of 1/5 (w/v). The reaction media consist of 50 mM ethanol, 1 mM CoA, 1 mM NAD^+, 1 mM TCEP in 0.15 M phosphate buffer pH 8. The reaction containing HB-4 additionally contained 100 mM glucose. The reaction containing HB-2.1 or HB-2.2 additionally contained 100 mM acetone. The enzymes and its amount present on each HB are defined in the Table S2.

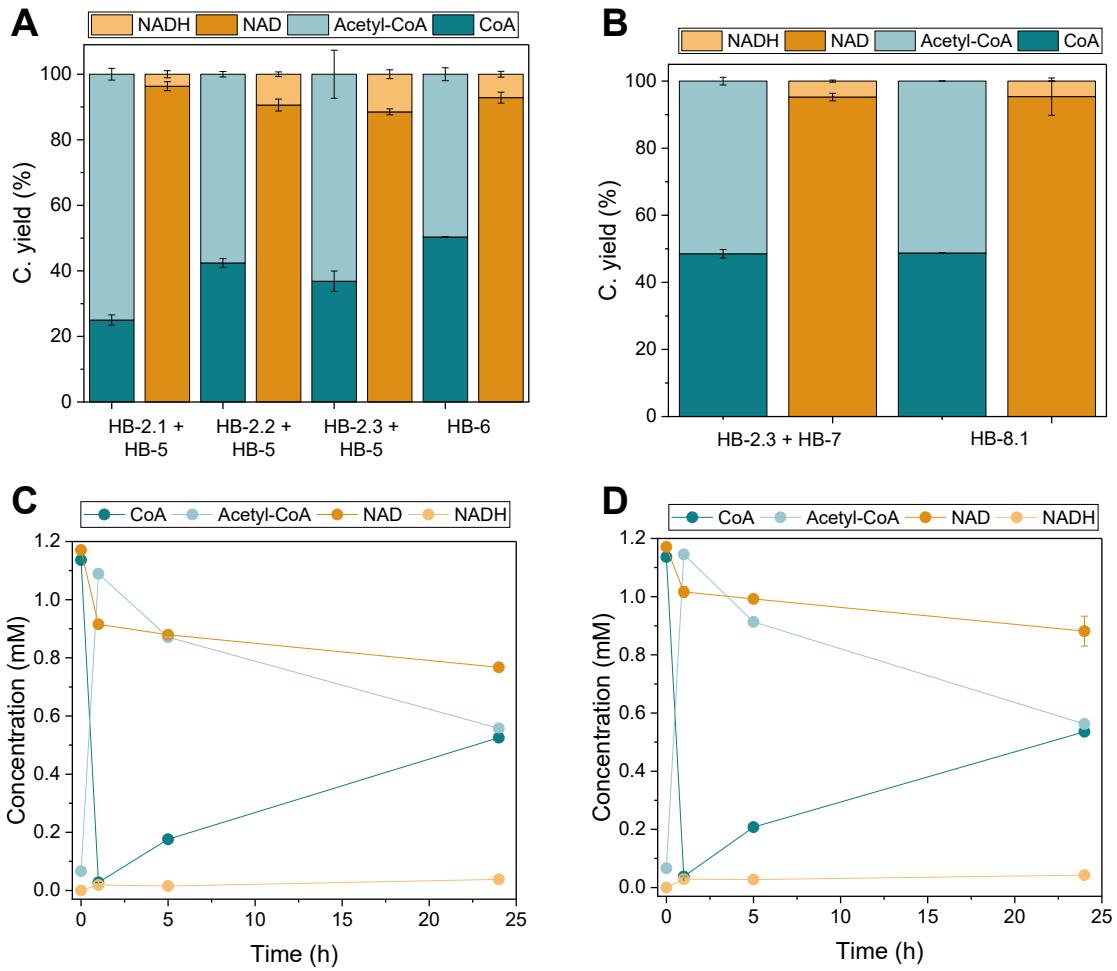

Figure S14. A) Relative cofactor concentrations from different combination of heterogeneous biocatalysts (HB) using AsTHL5 as thiolase. 25 mg of each HB were resuspended in the reaction mixture with a ratio 1/5 (w/v), containing 1 mM of NAD^+ and 1 mM CoA at pH 8 and 30º C. B) Relative cofactor concentrations from different combination of heterogeneous biocatalysts (HB) using ReTHL as thiolase. 25 mg of each HB were resuspended in the reaction mixture with a ratio 1/5 (w/v), containing 1 mM of NAD^+ and 1 mM CoA at pH 8 and 30º C. C) Time-course of the cofactors during the biosynthesis of 3-HBA from ethanol catalyzed the combination of HB-2.3 + HB-7. Reaction was done as indicated in B. D) Time-course of the cofactors during the biosynthesis of 3-HBA from ethanol catalyzed by HB-8.1. Reaction was done as indicated in B. The enzymes and its amount present on each HB are defined in the Table S2.

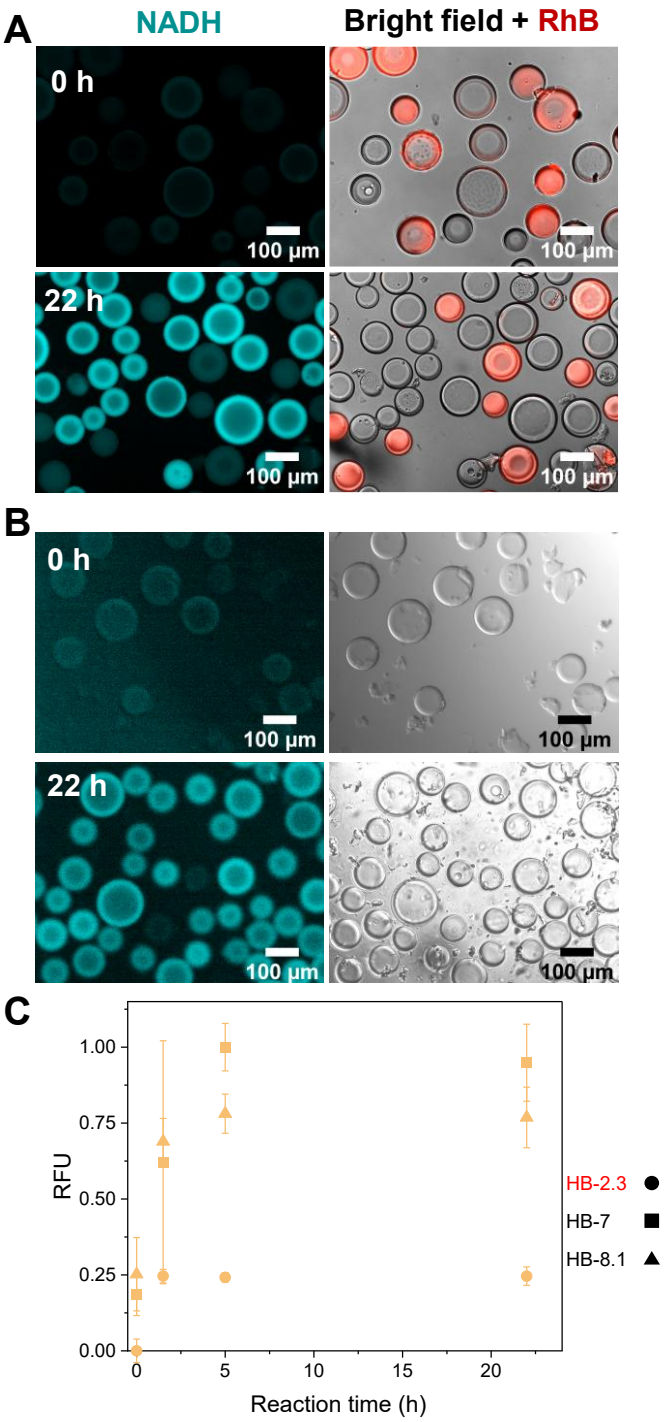

Figure S15: Epifluorescence microscopy images (left: blue channel, NADH autofluorescence; λ_{ex}: 385/30 nm; right: bright field and red channel particles labeled with Rhodamine B (RhB); λ_{ex}: 555/30 nm) tracking NADH along the reaction course. 25 mg of either a mix of HB-2.3 (labeled with RhB) and HB-7 (A), or unlabeled HB-8.1 (B) in a ratio 1/5 (w/v) of reaction mix. 5 µL samples were withdrawn from the reactor and analyzed under the microscope at 1.5, 5, and 22 hours of reaction (C). The RFU intraparticle intensity as a function of time. RFU values are the mean of from 8-10 particles and the error bars represents the corresponding standard deviation.

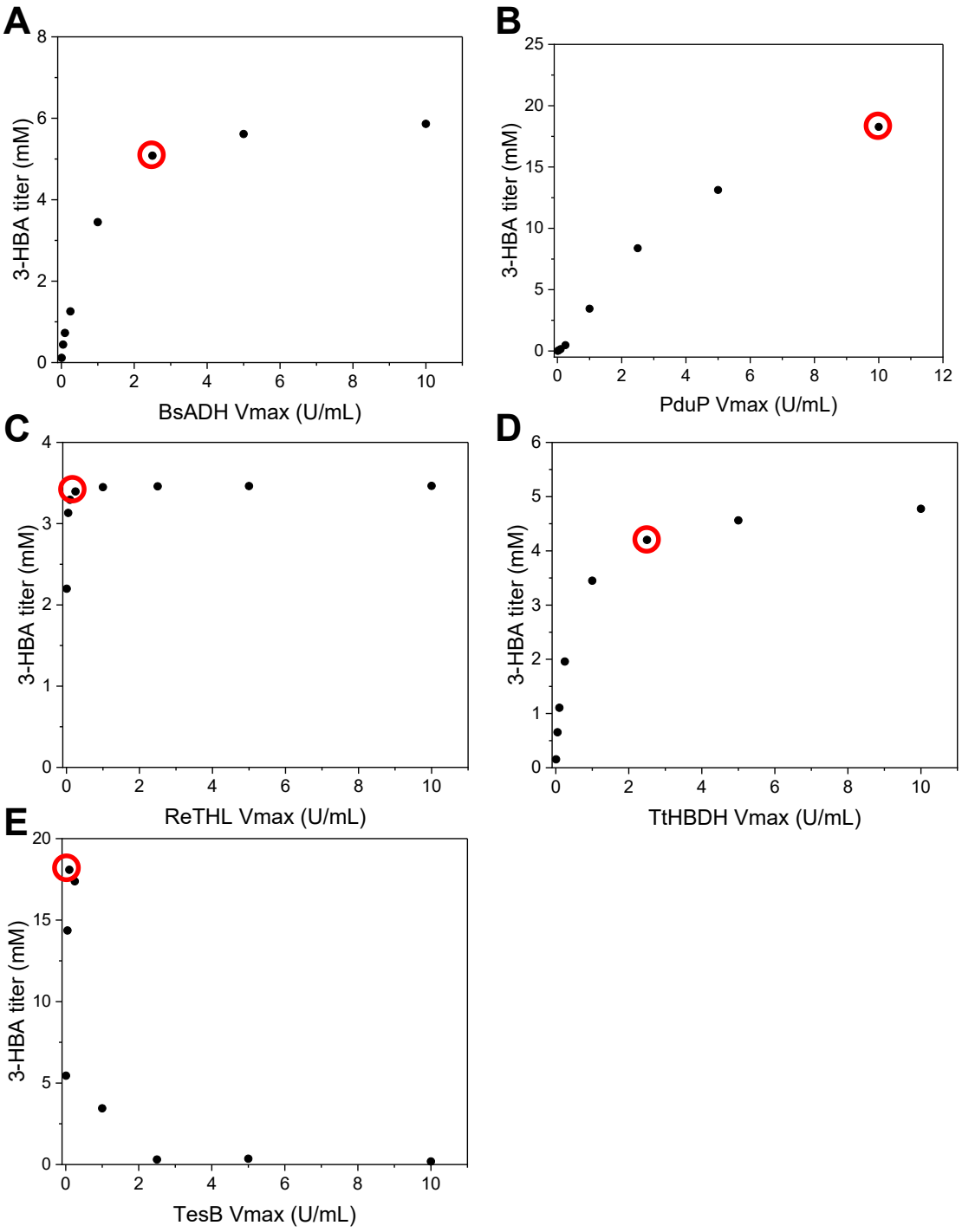

Figure S16: Optimization of enzyme concentration using Model 1.0. A) Parameter scan of BsADH V_{max} value. B) Parameter scan of ΔNPduP V_{max} value. C) Parameter scan of ReTHL V_{max} value. D) Parameter scan of TtHBDH V_{max} value. E) Parameter scan of EcTesB V_{max} value. Optimal V_{max} value of each enzyme is highlighted in a red circle. It is defined as the minimal V_{max} value that resulted in no less than 95% of the maximal 3-HBA titer at 24 hours achieved within the range of V_{max} for scanning. Details of the model construction and parameter scan method are described in the Methods section.

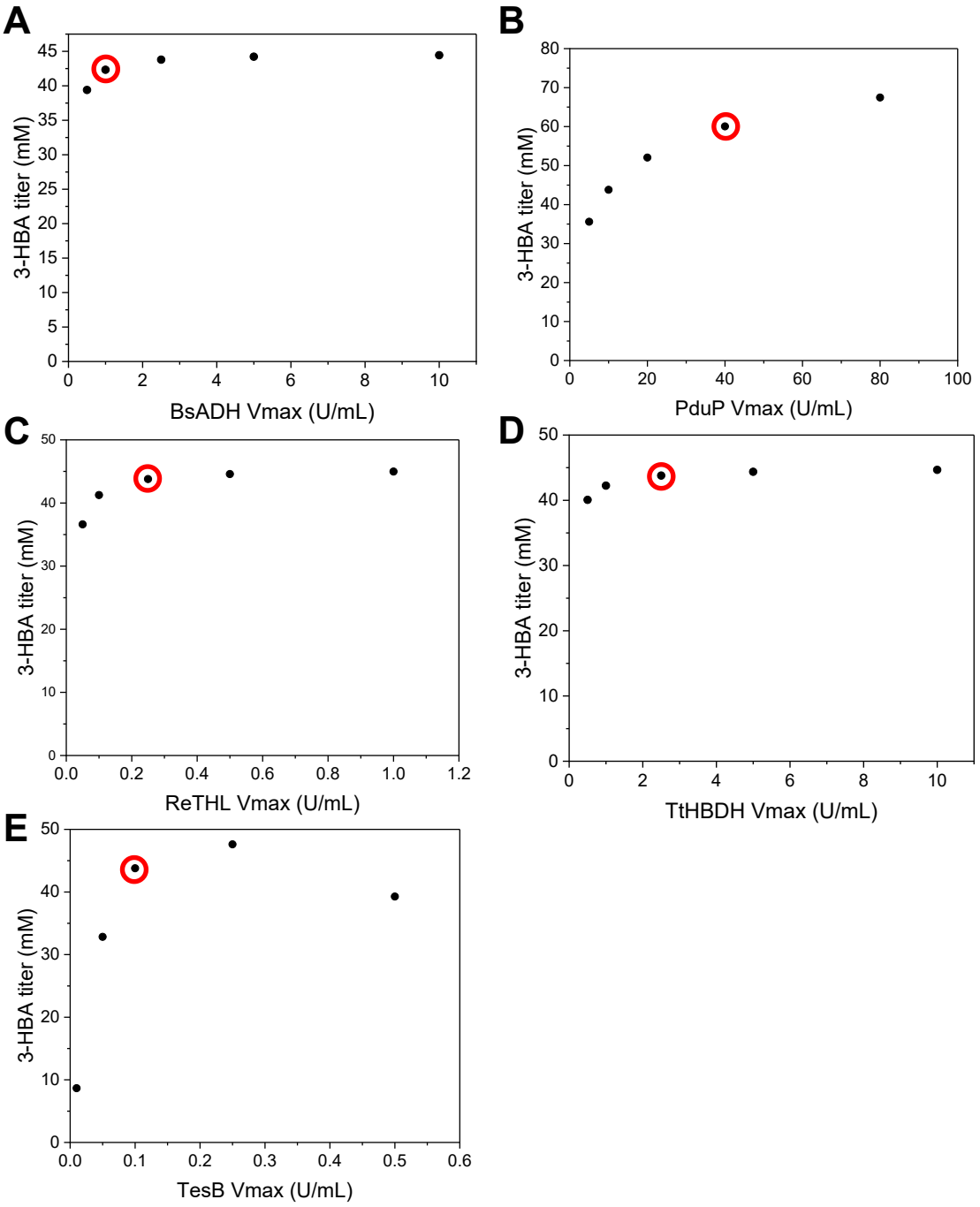

Figure S17: Optimization of enzyme concentration using Model 1.1. A) Parameter scan of BsADH V_{max} value. B) Parameter scan of ΔNPduP V_{max} value. C) Parameter scan of ReTHL V_{max} value. D) Parameter scan of TtHBDH V_{max} value. E) Parameter scan of EcTesB V_{max} value. The optimal V_{max} value of each enzyme is highlighted with a red circle. It is defined as the minimal V_{max} value that resulted in no less than 95% of the maximal 3-HBA titer at 24 hours achieved within the range of V_{max} for scanning. Details of the model construction and parameter scan method are described in the Methods section.

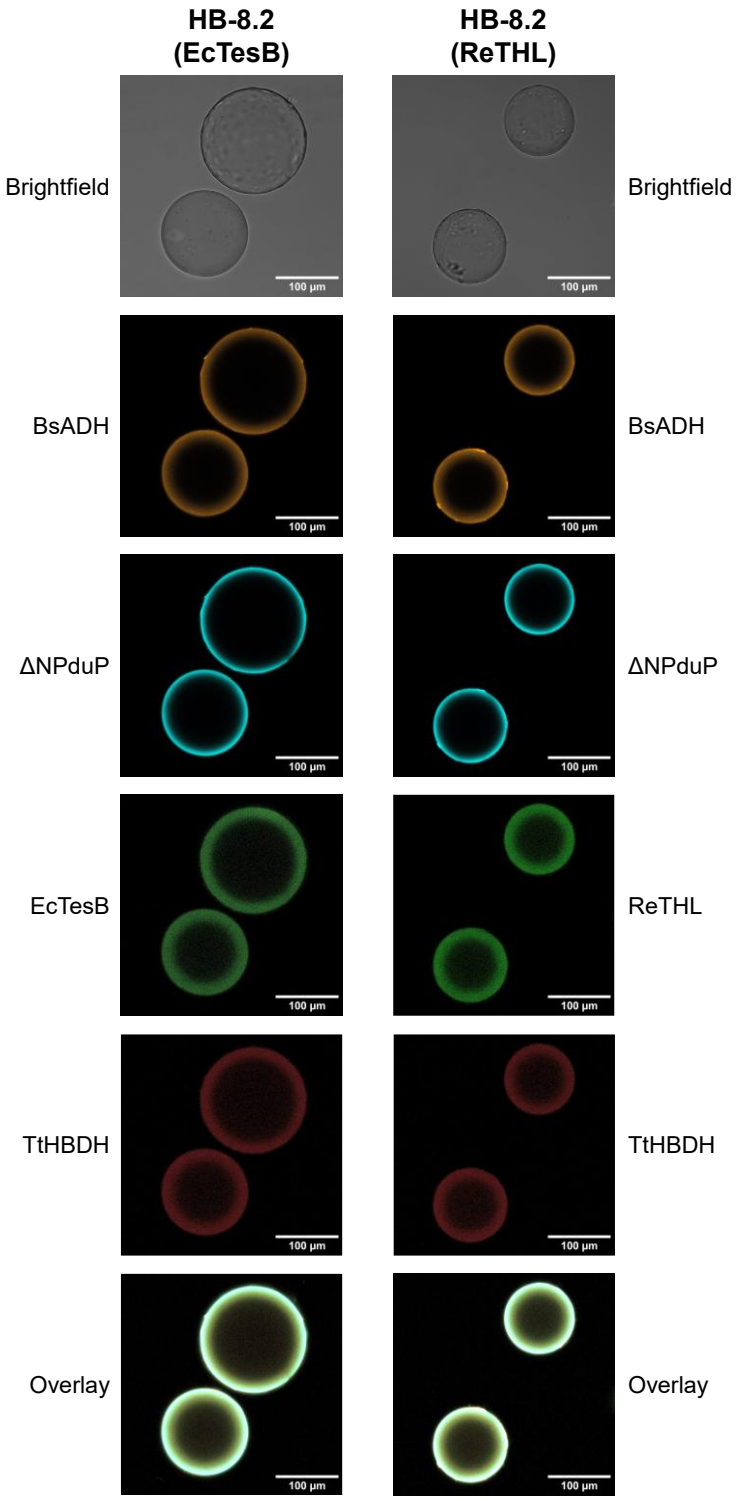

Figure S18: Confocal Laser Scanning Microscopy (CLSM) 40X images of HB-8.2 formed by one unlabeled enzyme (either ReTHL or EcTesB) and the left 4 enzymes labeled with compatible fluorophores; BsADH (RhB, λ_{ex}: 561 nm, orange color); ΔNPduP (Atto 390, λ_{ex}: 405 nm, blue color), either EcTesB or ReTHL (FTIC; λ_{ex}: 488 nm, green color) and TtHBDH (A647, λ_{ex}: 633 nm, red color), and overlay of all fluorescence channels obtained from HB-8.2.

A

Pearson coefficient	ReTHL labeled					
EcTesB labeled	Enzymes	BsADH	ΔNPduP	ReTHL	TtHBDH	EcTesB
	BsADH		0.79	0.29	0.24	-
	ΔNPduP	0.77		0.32	0.26	-
	ReTHL	-	-		0.12	-
	TtHBDH	0.27	0.30	-		-
	EcTesB	0.32	0.35	-	0.15	

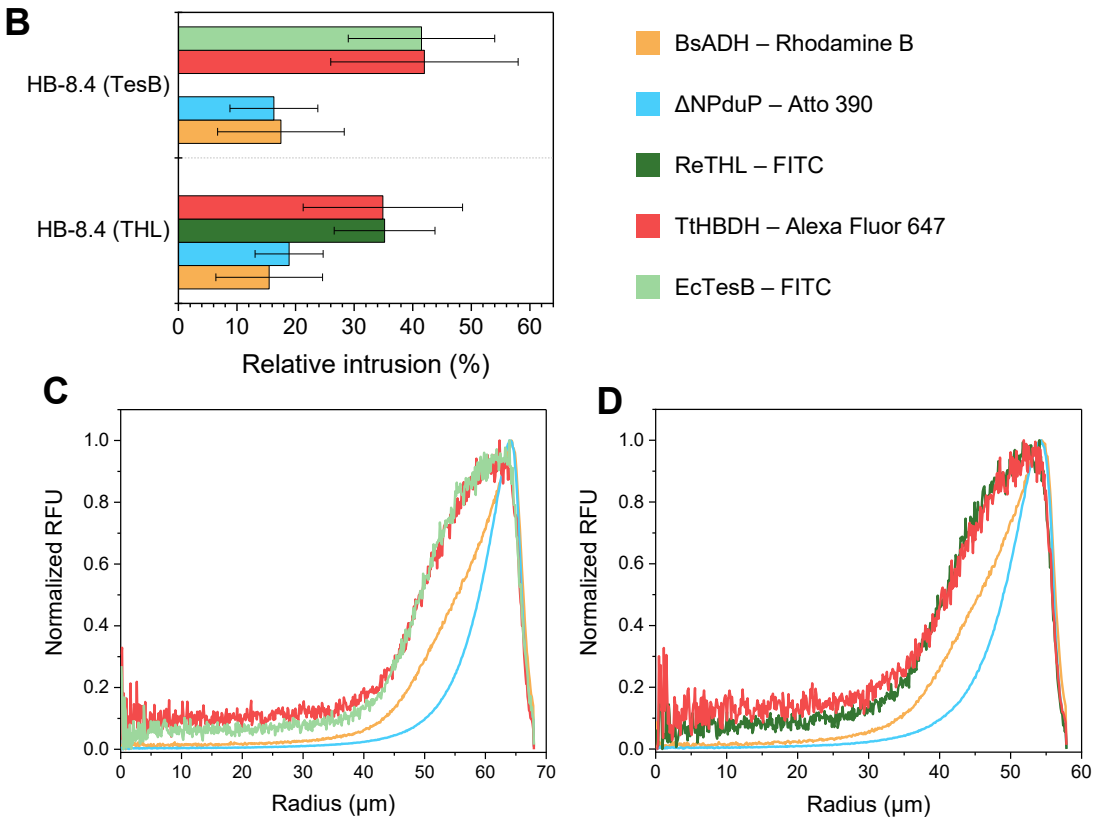

Figure S19: A) Pearson coefficient among the immobilized enzymes on HB-8.2, B) Relative infiltration of each enzyme through the radius of AG-G beads when co-immobilized. C) Normalized fluorescence intensity radial profile of HB-8.2 with ReTHL unlabeled. D) Normalized fluorescence intensity radial profile of the enzymes immobilized into HB-8.2 with EcTesB unlabeled. In A-D, data represent the mean value and standard deviation (error bars) of at least 15 microbeads.

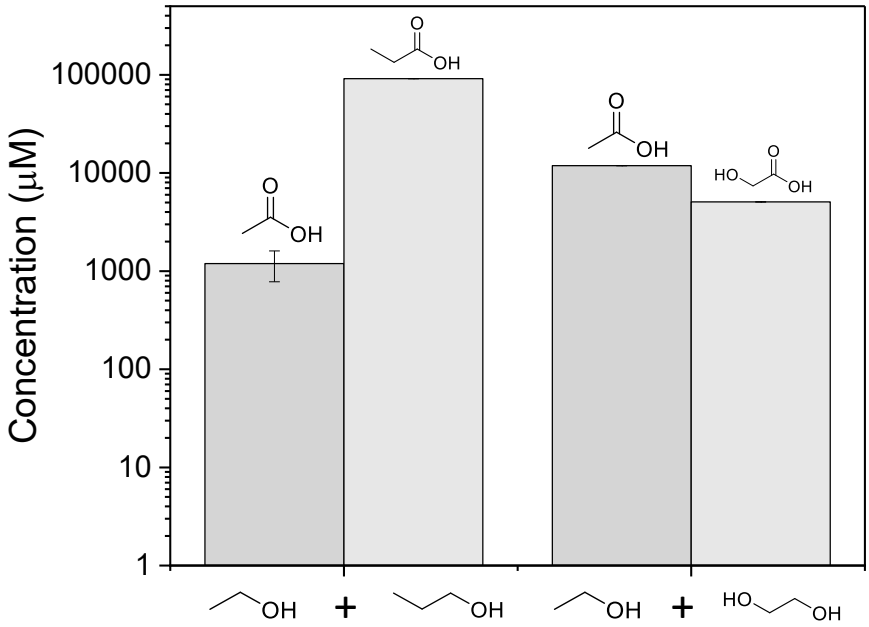

Figure S20. By-products concentration produced on the reactions starting from a mix of 20 mM ethanol and either 180 mM 1-propanol or 180 mM ethylene glycol in a molar ratio of 1:10. 40 mg of HB-8.2 were used on each reaction and resuspended in the corresponding reaction mix at a ratio of 1:5 (w/v).

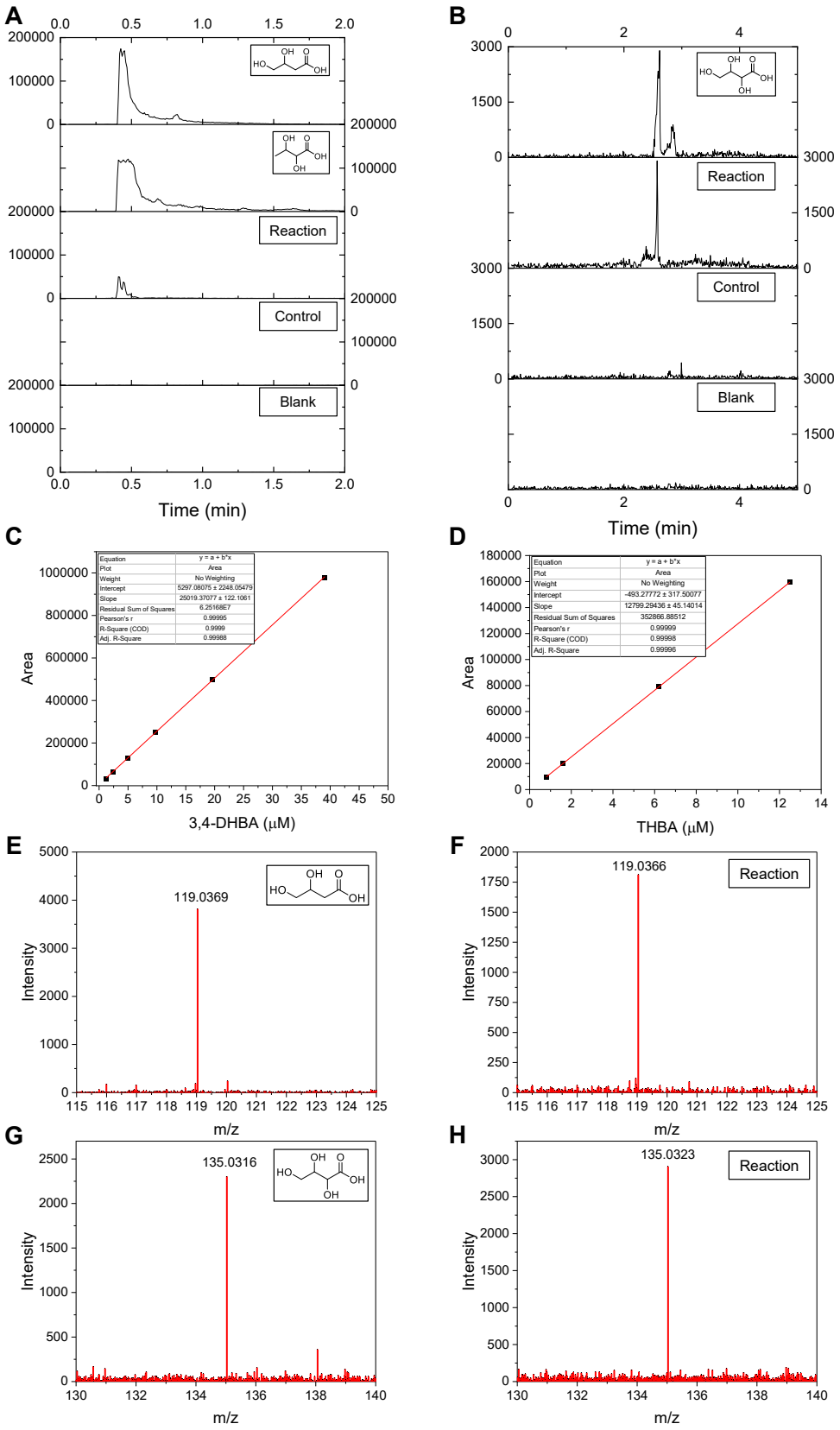

Figure S21. A) MS chromatograms of the 119.03±0.02 Da of different samples. B) MS chromatograms of the 135.03±0.02 Da of different samples. C) Calibration curve of 3,4-dihydroxybutyric acid. D) Calibration curve of 2,3,4-trihydroxybutyric acid (THBA). E) Mass spectra of 3,4-dihydroxybutyric acid injection at time 0.48 min. F) Mass spectra of the reaction at time 0.48 min. G) Mass spectra of 2,3,4-trihydroxybutyric acid injection at time 2.5 min. H) Mass spectra of the reaction at time 2.5 min.

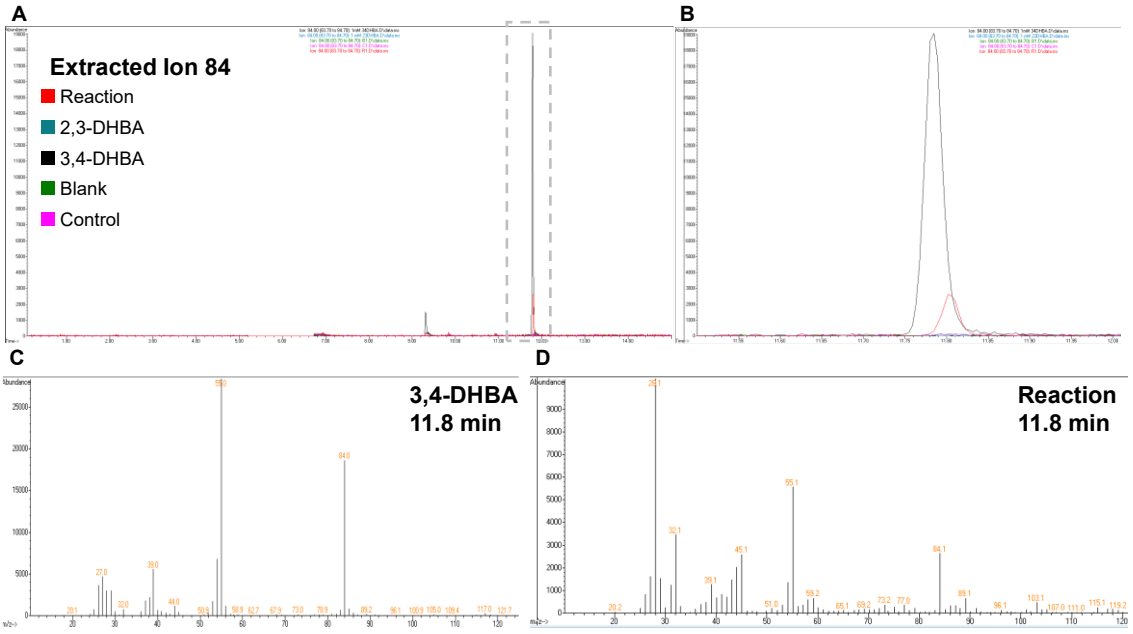

Figure S22. A) GC-MS chromatogram of the extracted Ion 84 is compatible with the double dehydration reaction of 3,4-dihydroxybutyric acid (3,4-DHBA). B) Zoom in on the GC-MS chromatogram at time 11.8 min. C) Mass spectra of 3,4-DHBA injection at 11.8 min. D) Mass spectra of the reaction at time 11.8 min.

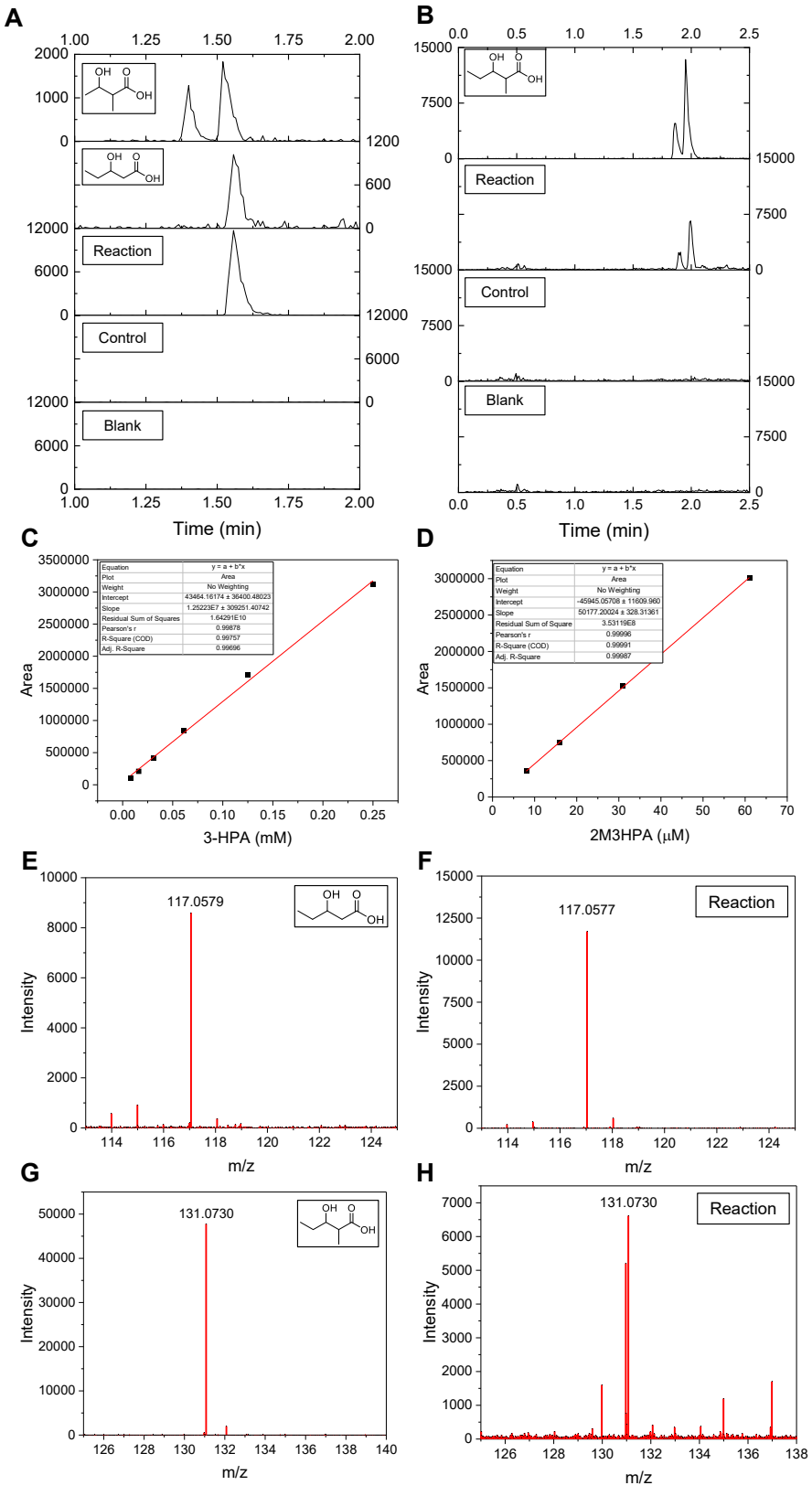

Figure S23. A) MS chromatograms of the 117.05±0.02 Da of different samples. B) MS chromatograms of the 131.05±0.02 Da of different samples. C) Calibration curve of 3-hydroxypentanoic acid (3-HPA). D) Calibration curve of 2-methyl-3-hydroxypentanoic acid (2M3HPA). E) Mass spectra of 3-hydroxypentanoic acid injection at time 1.56 min. F) Mass spectra of the reaction at time 1.56 min. G) Mass spectra of 3-hydroxy-2-methylpentanoic acid injection at time 2.0 min. H) Mass spectra of the reaction at time 2.0 min.

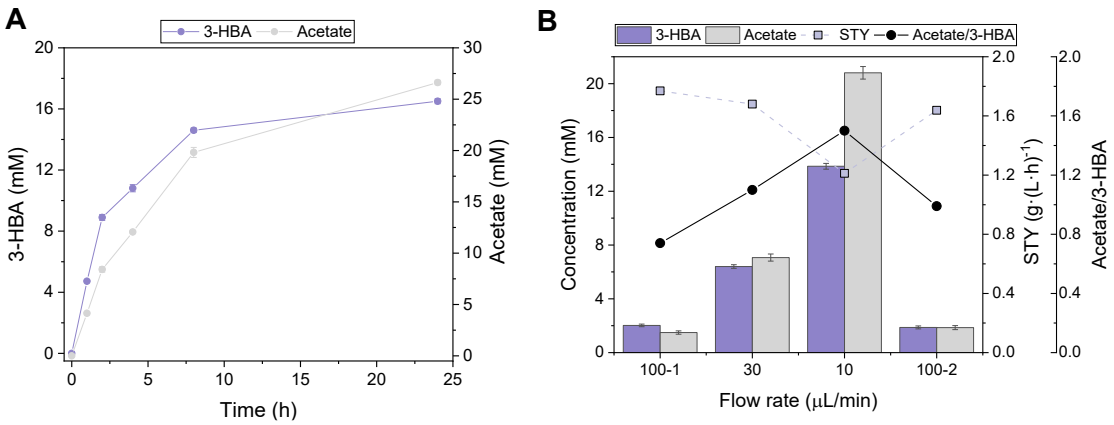

Figure S24. A) Time-course of the biosynthesis of 3-HBA (purple squares) and acetate (grey squares) with HB-8.2 from ethanol. Reactions were triggered by adding 3 mL of the reaction mixture over 600 mg of HB-8.2 in a ratio of 1/5 (w/v). Samples of the suspension were withdrawn over time, filtered, and analyzed as indicated in the Methods section. B) 3-HBA (Purple) and acetate (grey) titer and STY (light purple) regarding 3-HBA at different flow rates. Acetate/3-HBA molar ratio is represented in black dots.

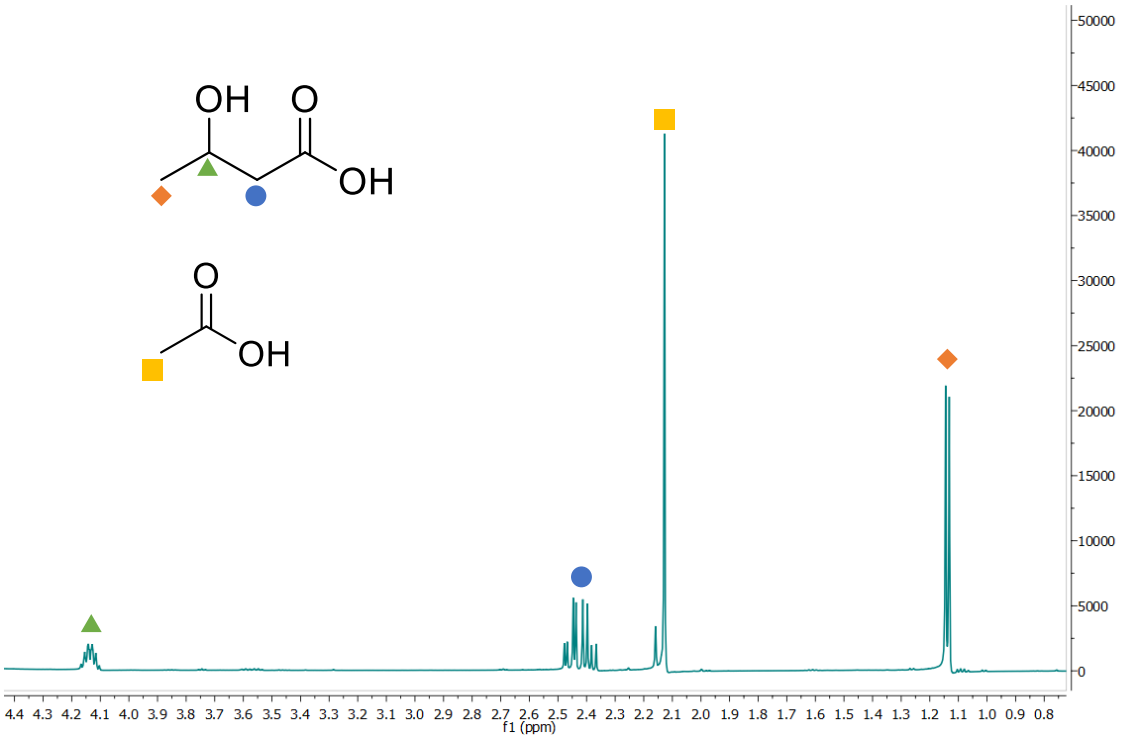

Figure S25. ^{1}H-NMR of isolated products through liquid-liquid extraction from the outcome solution of the PBR.

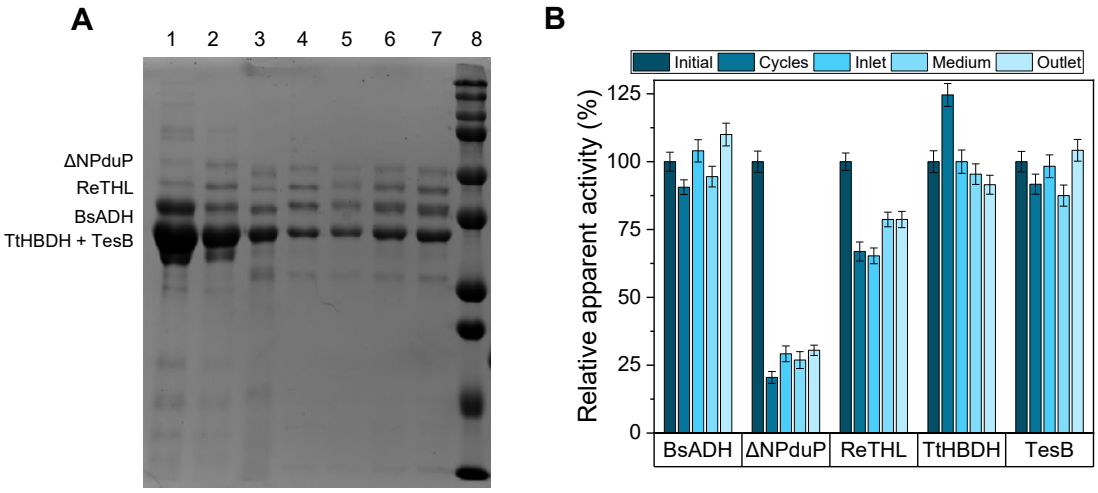

Figure S26. A) SDS-PAGE analysis of new and used HB-8.2, both in batch and in flow. Lane 1: Offered enzyme mix to AG-G. Line 2: Supernatant of the immobilization. Line 3: New HB-8.2. Line 4: HB-8.2 after 7 reaction cycles. Line 5: Inlet section of HB-8.2 after 25 days in flow. Line 6: Medium section of HB-8.2 after 25 days in flow. Line 7: Outlet section of HB-8.2 after 25 days in flow. Line 8 Molecular Weight Markers. B) Relative recovered activity of each enzyme on different samples of HB-8.2. The initial apparent activity of each enzyme after immobilization was taken as 100%.

Bibliography

1 Santiago-Arcos, J., Velasco-Lozano, S. & López-Gallego, F. Multienzyme Coimmobilization on Triheterofunctional Supports. *Biomacromolecules* **24**, 929-942 (2023). https://doi.org:10.1021/acs.biomac.2c01364